Supplemental materials:
Climate change increases the risk of false springs in European trees
OR
False spring risk increases across European trees in the face of climate change
OR
Heightened risk of false springs with climate change across six European tree species

Authors:

C. J. Chamberlain [1,2], B. I. Cook [3], I. Morales-Castilla [4,5] & E. M. Wolkovich [1,2,6]

Author affiliations:

[1]Arnold Arboretum of Harvard University, 1300 Centre Street, Boston, Massachusetts, USA;

[2]Organismic & Evolutionary Biology, Harvard University, 26 Oxford Street, Cambridge, Massachusetts, USA;

[3]NASA Goddard Institute for Space Studies, New York, New York, USA;

[4]GloCEE - Global Change Ecology and Evolution Group, Department of Life Sciences, Universidad de Alcalá, Alcalá de Henares, 28805, Spain

[5]Department of Environmental Science and Policy, George Mason University, Fairfax, VA 22030;

[6]Forest & Conservation Sciences, Faculty of Forestry, University of British Columbia, 2424 Main Mall, Vancouver, BC V6T 1Z4

*Corresponding author: 248.953.0189; cchamberlain@g.harvard.edu

Methods: Spatial predictor

Spatial autocorrelation (SA) is a common issue in spatial ecology given that nearby spatial units tend to be more similar than units far apart, and thus, cannot be considered as independent units, which is a frequent assumption in statistical tests (Diniz-Filho *et al.*, 2003). If model residuals are spatially autocorrelated, and thus, non-independent then model coefficients and errors may be biased in a hard-to-predict way (Mauricio Bini *et al.*, 2009). On the contrary, if model residuals are not autocorrelated, then SA should not be of concern (Hawkins, 2012).

To control for spatial autocorrelation and to account for spatially structured processes independent from our

environmental predictors of false springs, we generated an additional spatial predictor for the model. To avoid collinearity, we computed our spatial predictor from the residuals of a linear model of false springs as a function (Equation S1) of all other factors that are also spatially structured (e.g. spring temperature, altitude, distance to the coast), following the logic of spatial filter modelling (Diniz-Filho & Bini, 2005). The calculation of the spatial predictor followed the next steps: (a) we fit a linear model of false spring versus environmental factors, (b) we extracted the residuals of the regression Equation S1, which represent the portion of the variation in the number of false springs that is independent from the predictors in the model and (c) we utilized the residuals as our y_i values in a selection of spatial eigenvectors to retain only the minimal subset of spatial eigenvectors that are able to remove SA from model residuals. Specifically, we selected eigenvectors following the the minimization of Moran's I of the residuals (MIR) approach (Griffith & Peres-Neto, 2006; Diniz-Filho *et al.*, 2012; Bauman *et al.*, 2017). (d) Next, we fit a linear model between the residuals of Equation S1 and the subset of selected eigenvectors. And, finally, (e) we took the fitted values from this regression as our spatial predictor in our final model (see equation from main text, Equation 1), which can be interpreted as a latent variable summarizing the spatial structure in false springs that is unaccounted for by the rest of the environmental factors in our model (Morales-Castilla *et al.*, 2012). A spatial predictor generated in this way has three major advantages. First, it ensures that no SA is left in model residuals. Second, it avoids introducing collinearity issues with other predictors in the model. And third, it can be interpreted as a latent variable summarizing spatial processes (e.g. local adaptation, plasticity, etc.) occurring at multiple scales.

$$
\begin{aligned}
y_i = \alpha_{[i]} &+ \beta_{NAO_{[i]}} + \beta_{MST_{[i]}} + \beta_{Elevation_{[i]}} + \beta_{DistanceCoast_{[i]}} \\
&+ \beta_{ClimateChange_{[i]}} + \beta_{NAO \times Species_{[i]}} + \beta_{MST \times Species_{[i]}} + \beta_{Elevation \times Species_{[i]}} \\
&+ \beta_{DistanceCoast \times Species_{[i]}} + \beta_{ClimateChange \times Species_{[i]}} \\
&+ \beta_{NAO \times ClimateChange_{[i]}} + \beta_{MST \times ClimateChange_{[i]}} + \beta_{Elevation \times ClimateChange_{[i]}} \\
&+ \beta_{DistanceCoast \times ClimateChange_{[i]}} + \sigma_{[i]}
\end{aligned}
\tag{S1}
$$

Species rate of budburst calculations

Due to the paucity of data for BBCH 7 in the PEP725 dataset, we were unable to use observations for both budburst and leafout to determine the durations of vegetative risk. Instead, we used data from a growth chamber experiment (Flynn & Wolkovich, 2018) to determine the average number of days between budburst and leafout for our study species. We took the mean number of days between budburst and leafout for the entire experiment, which was 12 days. We compared this number to a field observation study (Donnelly *et al.*,

2017) that looked at the time between budburst and leafout across 10 species over 5 years. Finally, we assessed data that were provided by the USA National Phenology Network and the many participants who contribute to its Nature's Notebook program (USA-NPN,2019; www.usanpn.org/data/observational) for *Aesculus flava* (Sol.), *Aesculus glabra* (Willd.), *Alnus incana* (Moench.), *Betula nigra* (L.), *Betula papyrifera* (Marshall), *Fagus grandifolia* (Ehrh.), *Fraxinus americana* (L.), *Fraxinus nigra* (Marshall) and *Quercus velutina* (Lam.) and took the mean number of days between budburst and leafout. Across all three approaches, the average number of days between budburst and leafout was approximately 12 days.

Again, due to a lack of BBCH 7 data, we were unable to determine species-specific averages of number of days between budburst and leafout. We used a similar approach as above by using data from the growth chamber experiment (Flynn & Wolkovich, 2018) but instead of finding whole experiment means we determined species-specific averages. We used the rate of budburst of *Acer saccharum* (Marshall) for *Aesculus hippocastanum* (Buerki *et al.*, 2010), *Alnus incana* for *Alnus glutinosa*, *Betula papyrifera* for *Betula pendula* (Wang *et al.*, 2016), *Fagus grandifolia* for *Fagus sylvatica*, *Fraxinus nigra* for *Fraxinus excelsior* and *Quercus alba* (L.) for *Quercus robur* (Hipp *et al.*, 2017).

Results: The effects of climatic and spatial variation on false spring incidence

The overall model output estimates are for *Aesculus hippocastanum* as species were used as two-way interactions to simulate modeled groups on the main effects. The model estimates on the logit scale were converted to probability percentages for easier interpretation by using the 'divide by 4' rule (Gelman & Hill, 2006) and then back converted to the original scale.

References

Bauman D, Drouet T, Dray S, Vleminckx J (2017) Disentangling good from bad practices in the selection of spatial or phylogenetic eigenvectors. *Ecography*, **0**. doi:10.1111/ecog.03380.

Buerki S, Lowry II P, Alvarez N, Razafimandimbison S, Kupfer P, Callmander M (2010) Phylogeny and circumscription of *Sapindaceae* revisited: Molecular sequence data, morphology and biogeography support recognition of a new family, *Xanthoceraceae*. *Plant Ecology and Evolution*, **143**, 148–159. doi: 10.5091/plecevo.2010.437.

Diniz-Filho JAF, Bini LM (2005) Modelling geographical patterns in species richness using eigenvector-based spatial filters. *Global Ecology and Biogeography*, **14**, 177–185.

Diniz-Filho JAF, Bini LM, Hawkins BA (2003) Spatial autocorrelation and red herrings in geographical ecology. *Global ecology and Biogeography*, **12**, 53–64.

Diniz-Filho JAF, Bini LM, Rangel TF, Morales-Castilla I, Olalla-Tárraga MÁ, Rodríguez MÁ, Hawkins BA (2012) On the selection of phylogenetic eigenvectors for ecological analyses. *Ecography*, **35**, 239–249.

Donnelly A, Yu R, Caffarra A, *et al.* (2017) Interspecific and interannual variation in the duration of spring phenophases in a northern mixed forest. *Agricultural and Forest Meteorology*, **243**, 55–67.

Flynn DFB, Wolkovich EM (2018) Temperature and photoperiod drive spring phenology across all species in a temperate forest community. *New Phytologist*. doi:10.1111/nph.15232.

Gelman A, Hill J (2006) *Data analysis using regression and multilevel/hierarchical models*. Cambridge university press.

Griffith DA, Peres-Neto PR (2006) Spatial modeling in ecology: the flexibility of eigenfunction spatial analyses. *Ecology*, **87**, 2603–2613.

Hawkins BA (2012) Eight (and a half) deadly sins of spatial analysis. *Journal of Biogeography*, **39**, 1–9.

Hipp A, S Manos P, González-Rodríguez A, *et al.* (2017) Sympatric parallel diversification of major oak clades in the Americas and the origins of Mexican species diversity. *New Phytologist*, **217**. doi:10.1111/nph.14773.

Mauricio Bini L, Diniz-Filho JAF, Rangel TF, *et al.* (2009) Coefficient shifts in geographical ecology: an empirical evaluation of spatial and non-spatial regression. *Ecography*, **32**, 193–204.

Morales-Castilla I, Olalla-Tarraga MA, Purvis A, Hawkins BA, Rodriguez MA (2012) The imprint of cenozoic migrations and evolutionary history on the biogeographic gradient of body size in new world mammals. *The American Naturalist*, **180**, 246–256.

USA-NPN (2019) Plant and animal phenology data. *USA National Phenology Network*. doi: 10.5066/F78S4N1V. URL `http://doi.org/10.5066/F78S4N1V`.

Wang N, McAllister HA, Bartlett PR, Buggs RJA (2016) Molecular phylogeny and genome size evolution of the genus *Betula* (Betulaceae). *Annals of Botany*, **117**, 1023–1035. doi:10.1093/aob/mcw048.

Supplement: Tables and Figures

Table 1: Data collected from PEP725 for each species and the calculated number of false spring years

Species	Num. of Observations	Num. of False Springs	Num. of Sites	Num. of Years
Aesculus hippocastanum	156468	44746	10157	66
Alnus glutinosa	91094	27296	6775	65
Betula pendula	154897	46685	10139	66
Fagus sylvatica	129133	29237	9099	66
Fraxinus excelsior	92665	8256	7327	65
Quercus robur	131635	16657	8811	66

Table 2: Mean day of budburst and standard deviation for each species for before (1951-1983) and after climate change (1984-2016).

	1951-1983		1984-2016	
	mean	sd	mean	sd
Aesculus hippocastanum	102.2	12.44	95.35	12.09
Alnus glutinosa	102.8	14.81	94.90	14.71
Betula pendula	101.3	11.76	95.44	11.25
Fagus sylvatica	109.1	9.978	103.7	9.623
Fraxinus excelsior	119.4	11.79	113.5	11.53
Quercus robur	115.9	11.31	109.6	10.95

Table 3: Summary of main Bernouilli model of false spring risk without the species interactions (estimates presented on logit scale for *Aesculus hippocastanum*).

Term	Model Estimate	10%	25%	75%	90%
NAO Index	0.14	0.12	0.13	0.15	0.16
Mean Spring Temperature	-0.48	-0.50	-0.49	-0.47	-0.45
Distance from Coast	0.40	0.38	0.39	0.41	0.43
Elevation	0.19	0.16	0.18	0.20	0.22
Space Parameter	-0.06	-0.08	-0.07	-0.06	-0.05
Climate Change	0.35	0.33	0.34	0.36	0.37
NAO Index by Climate Change	-0.83	-0.85	-0.84	-0.82	-0.81
Mean Spring Temperature by Climate Change	0.42	0.40	0.41	0.43	0.44
Distance from Coast by Climate Change	-0.12	-0.15	-0.13	-0.11	-0.10
Elevation by Climate Change	-0.00	-0.03	-0.01	0.01	0.03
Space Parameter by Climate Change	-0.05	-0.07	-0.05	-0.04	-0.03

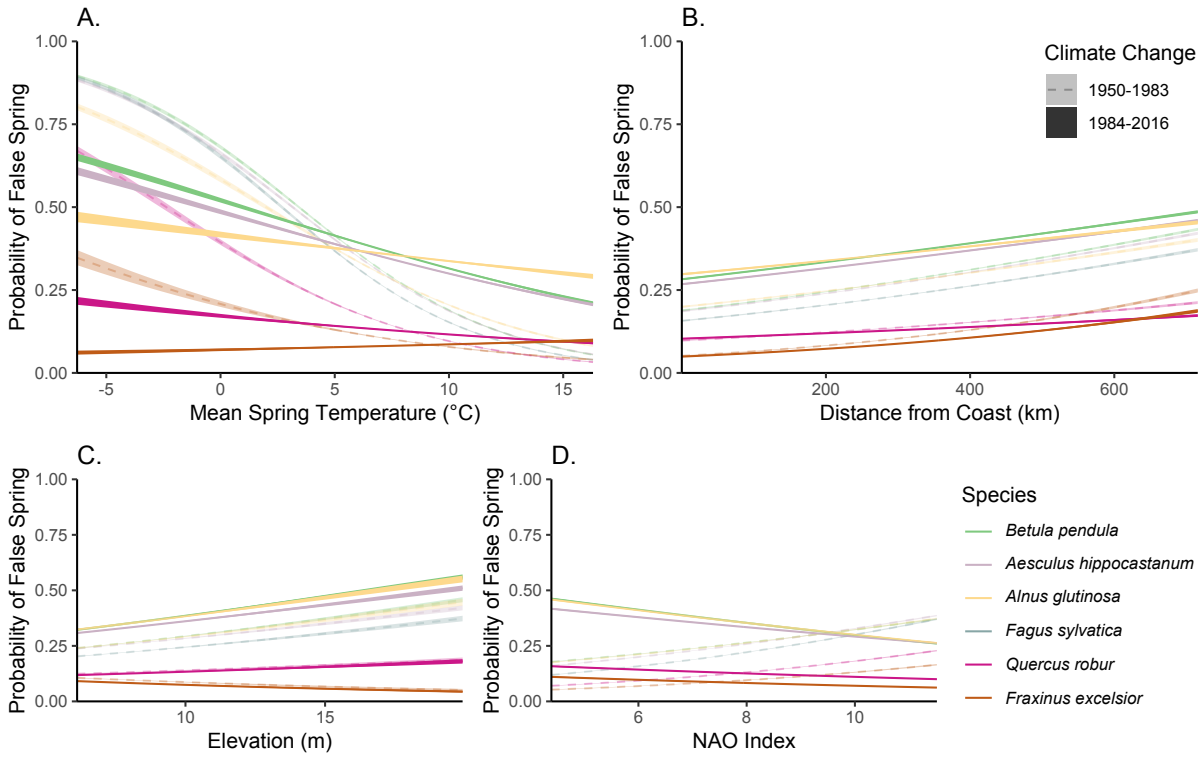

Figure 1: Average predictive comparisons for all climate change interactions with each of the main effects (i.e., mean spring temperature, distance from the coast, elevation, and NAO index) for all species.

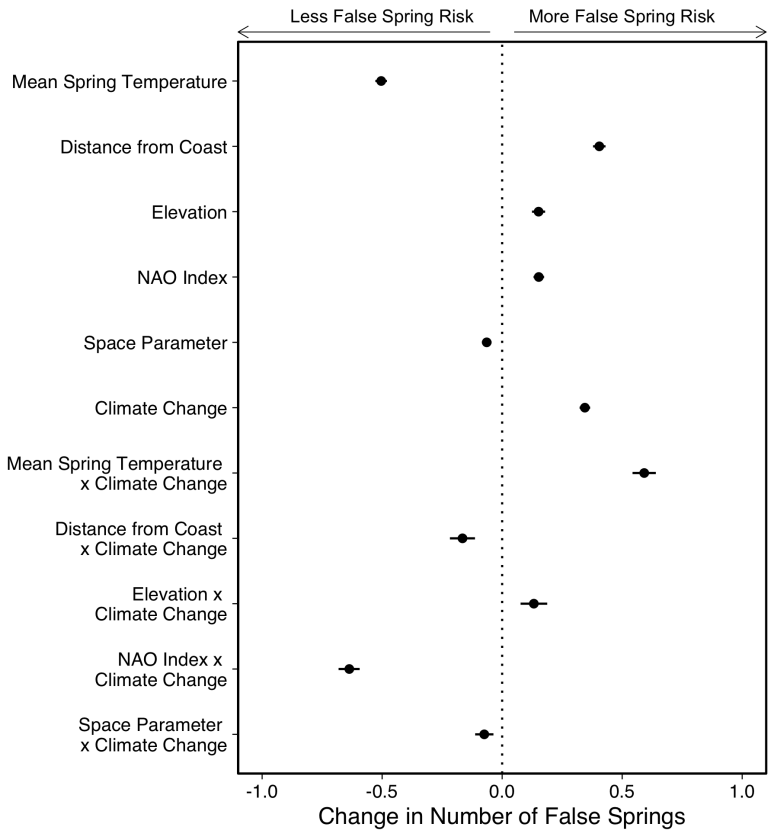

Figure 2: Model output with different durations of vegetative risk for each species. More positive values indicate an increased probability of a false spring whereas more negative values suggest a lower probability of a false spring. Dots and lines show means and 10% uncertainty intervals. Values closer to zero have less of an effect on false springs. There were 622,565 zeros and 132,463 ones for false springs in the data.

Table 4: Summary of Bernouilli model of false spring risk with varying durations of vegetative risk for each species without the species interactions (estimates presented on logit scale for *Aesculus hippocastanum*).

Term	Model Estimate	10%	25%	75%	90%
NAO Index	0.15	0.13	0.14	0.16	0.17
Mean Spring Temperature	-0.50	-0.53	-0.51	-0.49	-0.48
Distance from Coast	0.40	0.38	0.39	0.42	0.43
Elevation	0.15	0.12	0.14	0.16	0.18
Space Parameter	-0.06	-0.08	-0.07	-0.06	-0.04
Climate Change	0.34	0.32	0.34	0.35	0.37
NAO Index by Climate Change	-0.64	-0.68	-0.65	-0.62	-0.59
Mean Spring Temperature by Climate Change	0.59	0.54	0.57	0.61	0.64
Distance from Coast by Climate Change	-0.17	-0.22	-0.19	-0.14	-0.11
Elevation by Climate Change	0.13	0.08	0.11	0.15	0.19
Space Parameter by Climate Change	-0.07	-0.11	-0.09	-0.06	-0.04

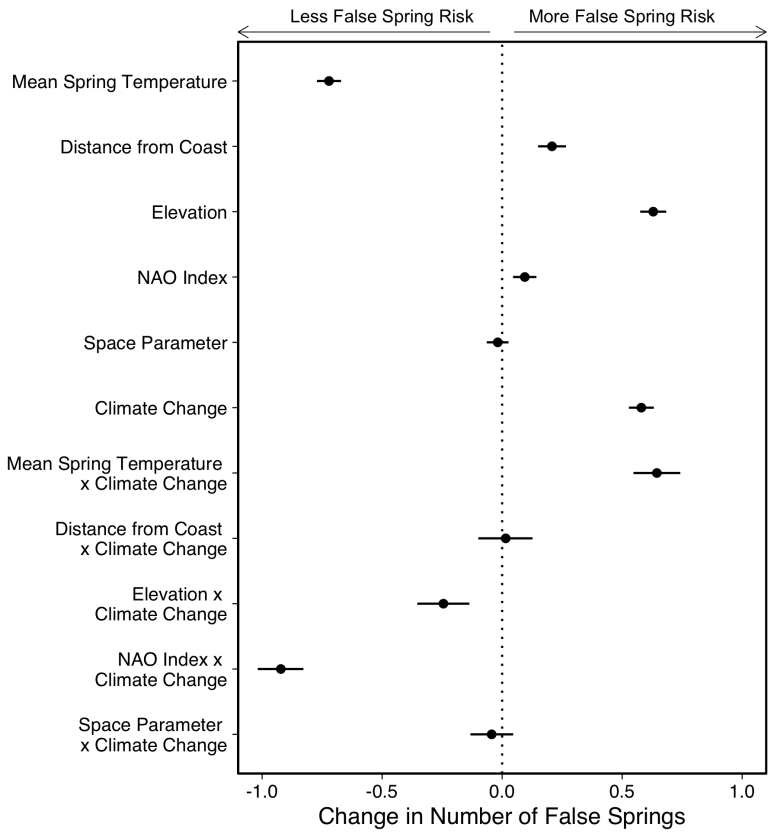

Figure 3: Model output with a lower temperature threshold (-5°C) for defining a false spring. More positive values indicate an increased probability of a false spring whereas more negative values suggest a lower probability of a false spring. Dots and lines show means and 10% uncertainty intervals. Values closer to zero have less of an effect on false springs. There were 730,996 zeros and 23,855 ones for false springs in the data.

Table 5: Summary of Bernouilli model of false spring risk with a lower temperature threshold (-5°C) for defining a false spring without the species interactions (estimates presented on logit scale for *Aesculus hippocastanum*).

Term	Model Estimate	10%	25%	75%	90%
NAO Index	0.09	0.05	0.07	0.11	0.14
Mean Spring Temperature	-0.72	-0.77	-0.74	-0.70	-0.67
Distance from Coast	0.21	0.15	0.18	0.23	0.27
Elevation	0.63	0.58	0.61	0.65	0.68
Space Parameter	-0.02	-0.06	-0.04	0.00	0.03
Climate Change	0.58	0.53	0.56	0.60	0.63
NAO Index by Climate Change	-0.92	-1.02	-0.96	-0.88	-0.83
Mean Spring Temperature by Climate Change	0.64	0.55	0.60	0.69	0.74
Distance from Coast by Climate Change	0.01	-0.10	-0.03	0.06	0.13
Elevation by Climate Change	-0.24	-0.35	-0.29	-0.20	-0.14
Space Parameter by Climate Change	-0.04	-0.13	-0.08	-0.01	0.05